Proceedings of the 6th Asian Geothermal Symposium, Oct. 26-29, 2004
Mutual Challenges in High- and Low- Temperature Geothermal Resource Fields, 39-46

MEASUREMENT OF GROUNDWATER TEMPERATURE FOR UNDERGROUND THERMAL UTILIZATION

Kasumi YASUKAWA[1], Youhei UCHIDA[1], Norio TENMA[1], Somkid BUAPANG[2] and Hirofumi MURAOKA[1]
[1]GSJ/AIST, AIST Tsukuba Central 7, Tsukuba, Ibaraki 305-8567, Japan
[2]Department of Groundwater Resource, Thailand
e-mail: kasumi-yasukawa@aist.go.jp

ABSTRACT

For promotion of geothermal heat-pump systems in Asia, especially at moderate to tropical climate regions, it is important to understand the subsurface temperature distribution in populated areas. Subsurface temperature distribution in the Sendai plain was obtained by field measurements and numerical modeling of the groundwater flow. In this region, geothermal heat-pump can be applied for both space heating and cooling. For the region along the Chao-Phraya river in Thailand, results of temperature measurement in observation wells suggests that geothermal heat-pump may be applied for space cooling in the upper basin, but not in the lower one. Thus the possible potential geothermal heat-pump application at any location can be judged by comparing the subsurface and atmospheric temperatures. The final goal of our project is to make potential map of heat resources in major plains in East Asia for geothermal heat-pump application.

Keywords: geothermal heat-pump, groundwater flows, numerical simulation, Sendai plain, Chao-Phraya river

1. INTRODUCTION

Direct use of geothermal energy, especially geothermal heat-pump application has extensively grown in Europe and the U. S. A. in recent two decades. Geothermal heat-pump may achieve higher coefficient of performance than conventional air-source heat-pumps that results in energy (electricity) savings and protection of the environment. However, the current number of its installation in Asian countries is quite limited. In eastern Asian countries, where significant economical growth in this century is expected, energy saving and environmental protection will be major matters of importance. Therefore, rapid growth of geothermal heat-pump installation is desirable.

Geothermal heat-pump system can be applied for both/either space heating and/or cooling depending on surface and underground temperature conditions. Since it has been intensively installed in western developed countries, which have rather cold climates, it is known as “applicable to anywhere in the world”. It is true to cold to moderate climate regions, but may not be true for tropical regions where the atmospheric temperature is almost stable through a year. Although space cooling is important at the tropics, underground temperature may always be higher than atmospheric temperature and there is no thermal merit of geothermal heat-pump system. However, still there is a possibility of thermal merit for tropical regions if the cooling effect of groundwater flow is locally dominant than the heating effect of heat flux from a depth.

Thus mapping of local underground temperature distribution may be the first step for an intensive installation of geothermal heat-pump system. Since the underground thermal regime is largely affected by groundwater flows, to understand the flow patterns of the groundwater at each study area is essential. For this purpose, we measured the underground temperature, hydraulic head, and chemical and isotopic components of the water at observation wells in some model fields. These data at observation points will be interpolated by numerical simulation to get three dimensional temperature distribution. This paper shows the procedures of data acquisition and numerical modeling at model fields. The final aim of our study is to make a map of East Asia that indicates the available type of geothermal heat-pump system at any arbitrary location based on the surface and subsurface temperature conditions.

2. SUBSURFACE TEMPERATURE

Subsurface temperature at a depth of 20-30 m or deeper is stable through a year and generally higher than average temperature (in time) of its corresponding ground surface. Figure 1 schematically shows subsurface temperature profile for different climate regions when the heat conduction from a depth is dominant (no groundwater flow). Figure 2 shows time variation of subsurface (at depths of 30-50 m) and atmospheric temperature for climates corresponding to Figure 1. For cold climate region, subsurface temperature is mostly higher than atmospheric one, so that the utilization of geothermal heat-pump is quite suitable for space heating. For moderate climate region, such as in Tokyo, subsurface temperature is higher in the winter and lower in the summer, so that geothermal heat-pump is useful for both space heating and cooling. For tropics, where space cooling is preferred, subsurface temperature is higher or approximately equal to atmospheric one and no thermal merit of geothermal heat-pump can be seen.

However, groundwater flow, which is controlled by topographies of the ground surface and the subsurface boundaries where permeability drastically changes, may perturb the subsurface thermal regime. Figure 3 shows the observed subsurface temperature at a N-S cross-section in Nobi plain, Japan (Uchida and Sakura, 1999). In this plain, groundwater recharged at north slowly flows southward, due to the geometries of the surface and the boundary between Quarternary and Tertiary.

While ground water lingers in subsurface layers, it is gradually heated by heat flow from a depth. As a result, subsurface temperature at discharge zone is higher than at recharge zone at same depth. Such temperature difference is approximately 3 to 5 K at the Nobi plain. This phenomenon is shown in Figure 4 as different types of temperature profiles. Thus temperature change of few K from the temperature shown in Figure 2 may be achieved by groundwater flow and thermal merit of geothermal heat-pump for tropics may occur. Therefore understanding of subsurface temperature distribution is significantly important to judge which kind of subsurface thermal utilization is possible or not at local districts.

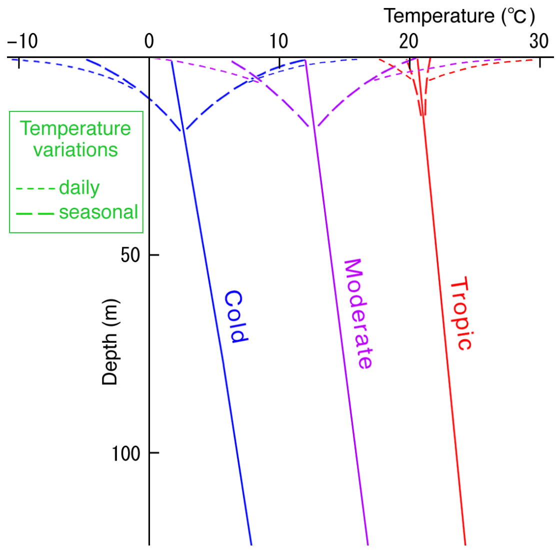

Figure 1. Conceptual profile of subsurface temperature.

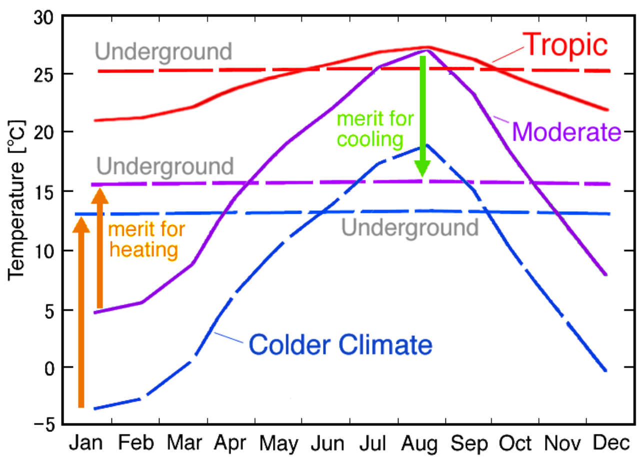

Figure 2. Time variation of subsurface (dashed lines) and atmospheric (solid lines) temperature.

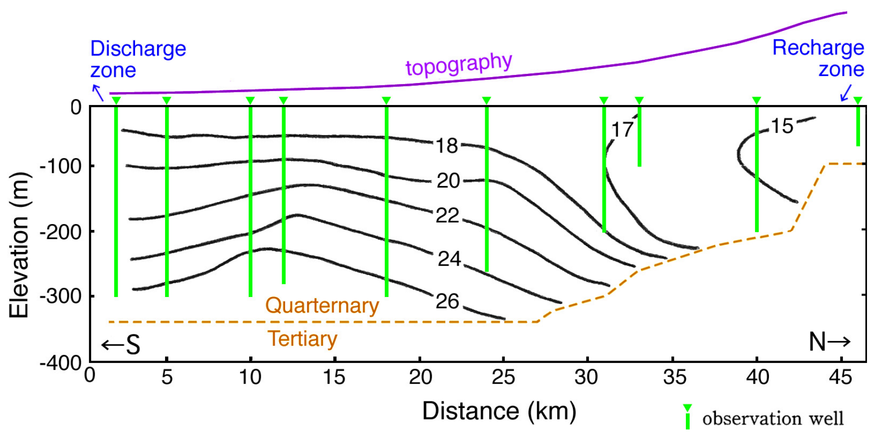

Figure 3. Isotherms of subsurface temperature observed along N-S cross-section at the Nobi plain (Uchida and Sakura, 1999).

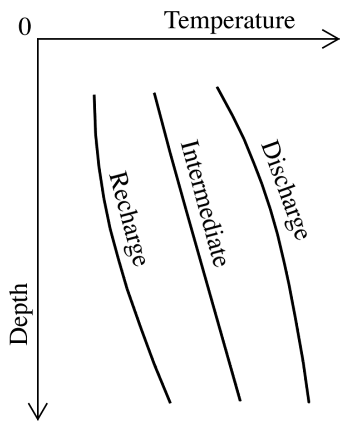

Figure 4. Types of temperature profiles affected by groundwater flow.

3. METHODS FOR UNDERSTANDING SUSBSURFACE TEMPERATURE DISTRIBUTION

In this section, the procedure to understand subsurface temperature distribution at a plain or a basin will be introduced with a case study at the Sendai plain (Figure 5), Tohoku, Japan, as an example of moderate climate area.

The distance between mountainous discharge area in the west and recharge zone in the east is merely 10 km here. Modern development of Sendai area had caused serious influences on groundwater system such as subsidence and inflow of seawater. Since the local authorities imposed limit for groundwater use, the water level has been recovered.

Figure 6 shows the sampling points for chemical and isotope analysis and temperature measurements (left), and resultant temperature distribution at an elevation of –50m (right). The temperature at a certain elevation is higher in the west because the same elevation corresponds to deeper part at mountainous region.

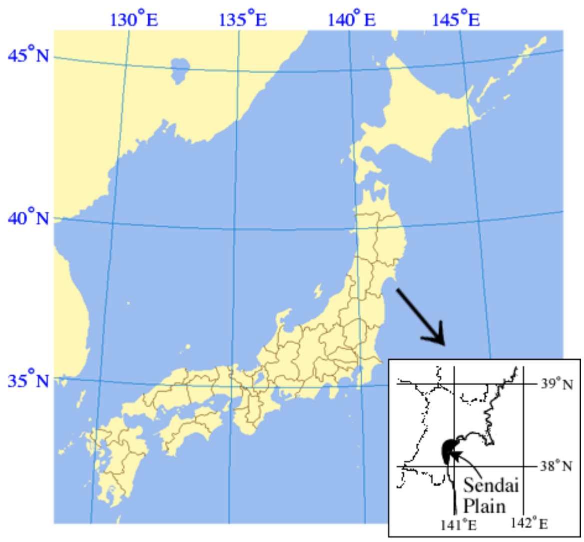

Figure 5. Location of the study area.

Figure 7 shows the isotopic ratio of the water samples. The precipitation at highland generally has higher ratio of lighter isotopes while that in lowland does heavier ones. Figure 7 suggests that lighter rainfalls in highland infiltrate into deeper part to flow in Tertiary layers while that in lowland merely does in shallower Quarternary layers, as is schematically shown in Figure 8.

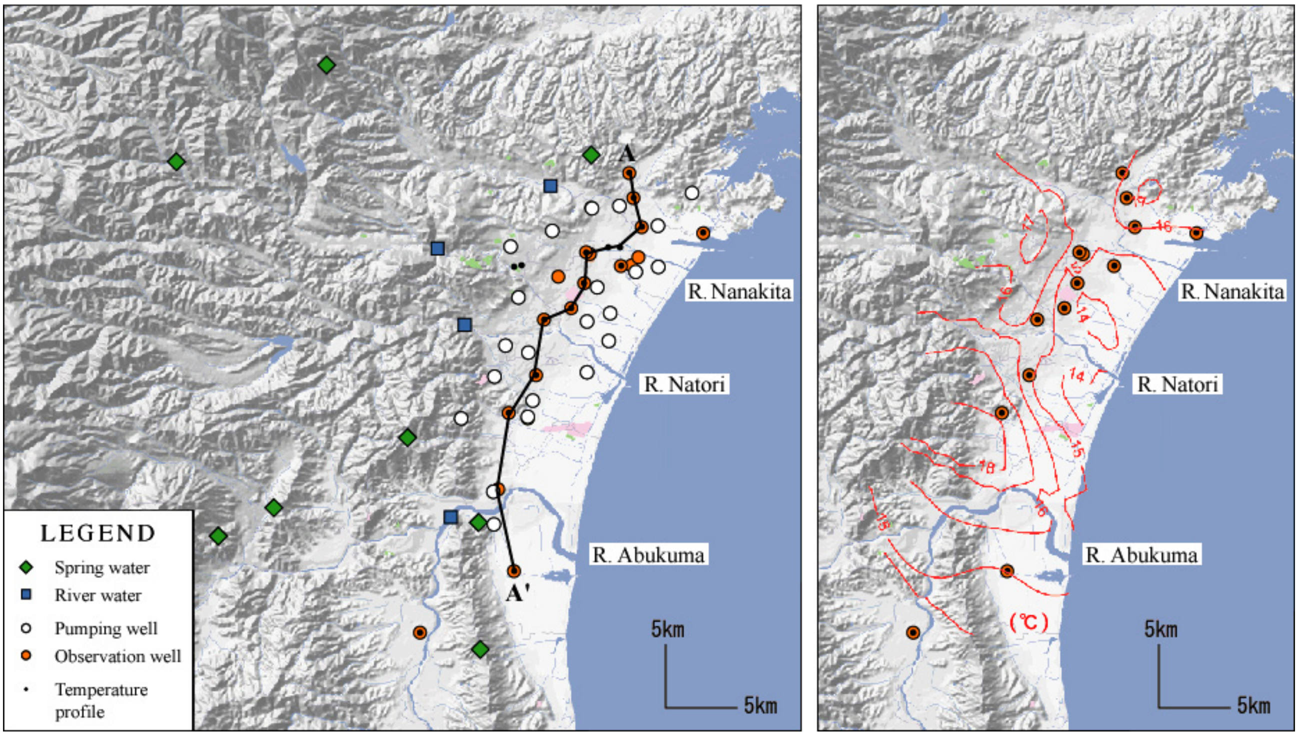

Figure 6. Sampling points (left) and resultant contour map of isotherms at an elevation of –50m (right).

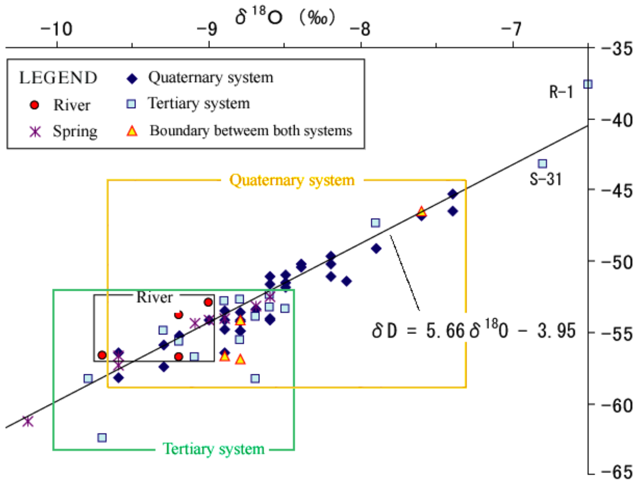

Figure 7. Isotope components of the samples in the Sendai plain.

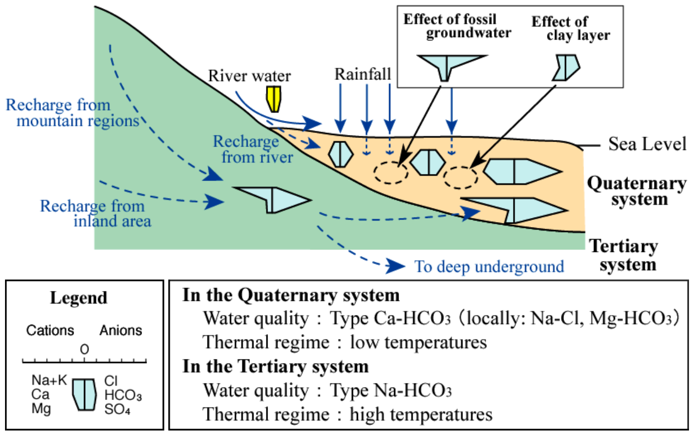

Figure 8. Schematic subsurface flow model in the Sendai plain.

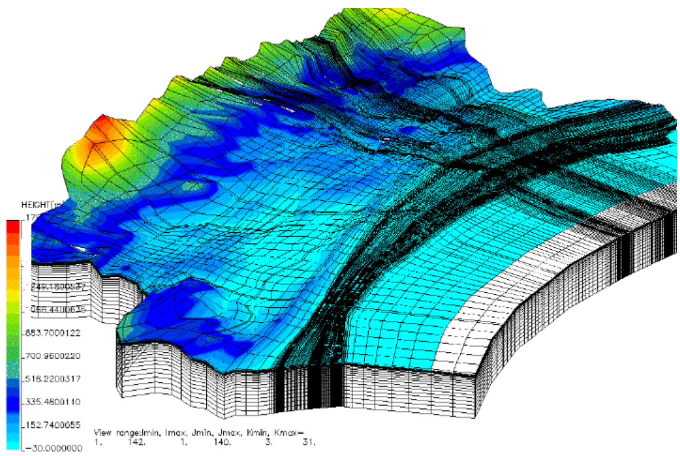

Figure 9a. Mesh for 3D modeling (3D image).

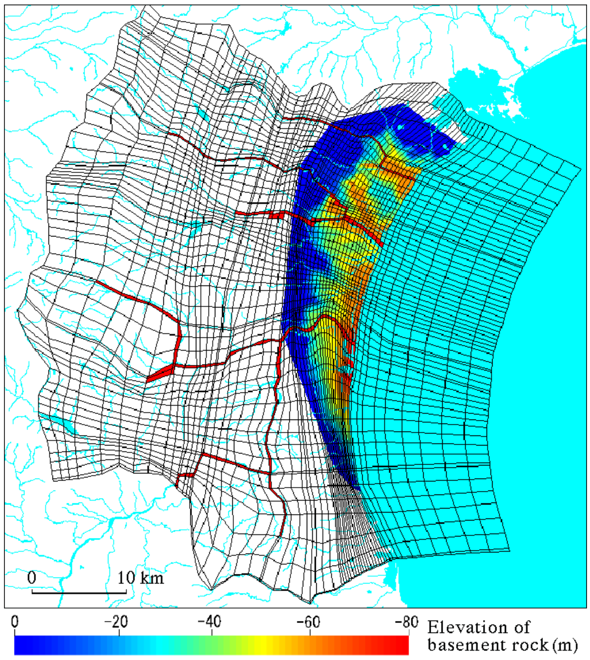

Figure 9b. Mesh for 3D modeling (plan view).

In order to quantitatively confirm the conceptual model and reconstruct the subsurface flow system in the whole region, a numerical simulation was conducted. The applied simulation code is GETFLOWS (GEneral purpose Terrestrial FLOW Simulator, by Geosphere Environmental Technology Corp.). The governing equations in GETFLOWS are mass conservation equation for each component and energy conservation equations for liquid and solid phases (Table 1).

The simulated area is approximately 60 x 60 km2. The number of grid mesh is 19,599 in plan view and 587,970 in total (Figure 9). Simulation starts with empty (dry) condition of the system. Then rainfall of 1.71 mm/day, which is based on the annual precipitation at Sendai, starts at t=0. The extents of saturated and unsaturated zones, existence of rivers will be automatically reconstructed through calculation. Rock parameters are given for each grid block according to the rock type (Quaternary or Tertiary), as shown in Table 2. The bottom temperature is kept 79°C, while atmospheric one was kept 14.5°C, based on the meteorological data. Calculation was continued till the system reaches to a steady state.

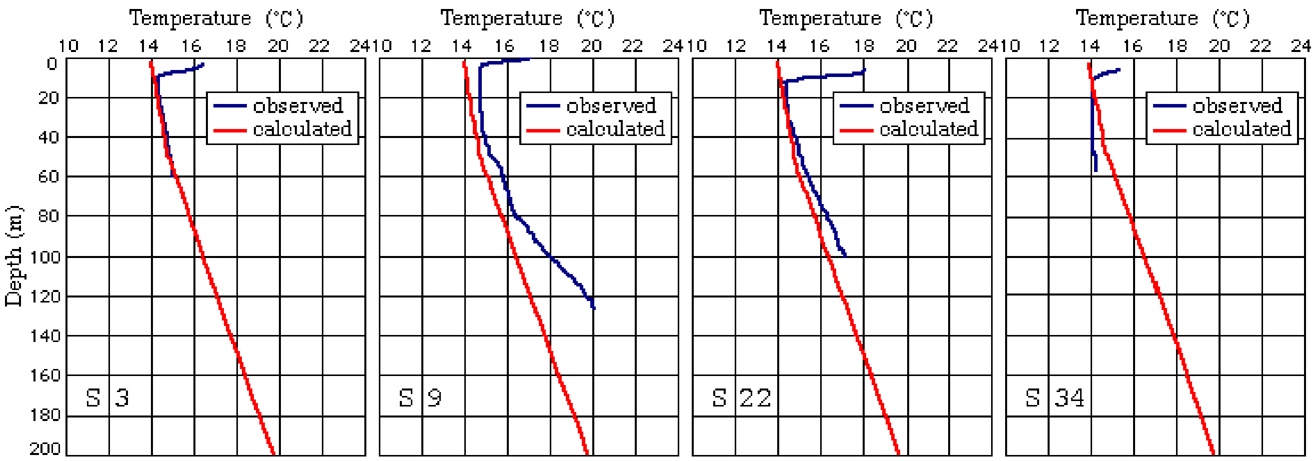

Figure 10. Calculated and observed temperature profiles in wells.

Table 1. Governing equations in GETFLOWS (Mori et al, 2003)

Mass conservation	① Water	$\nabla\left(\frac{Kkr_{cw}}{\mu_{cw}B_{cw}}\nabla\Psi_{cw}\right)+\nabla\left(\frac{Kkr_{cc}}{\mu_{cc}B_{cc}}\nabla\Psi_{cc}\right)-q_{wS}^{cw}-q_{wS}^{cc}=\frac{\partial}{\partial t}\left(\phi\frac{S_{cw}}{B_{cw}}+\phi\frac{S_{cc}}{B_{cc}}\right)$
	② Air	$\nabla\left(\frac{Kkr_{ca}}{\mu_{ca}B_{ca}}\nabla\Psi_{ca}\right)-q_{caS}=\frac{\partial}{\partial t}\left(\phi\frac{S_{ca}}{B_{ca}}\right)$
	③ NAPL	$\nabla\left(\frac{Kkr_{cc}R_{cc}}{\mu_{cc}B_{cc}}\nabla\Psi_{cc}\right)-q_{cS}^{cc}-f_{cS}^{cc-cw}-f_{cS}^{ca-cc}-f_{cS}^{cc-r}=\frac{\partial}{\partial t}\left(\phi\frac{S_{cc}R_{cc}}{B_{cc}}\right)$
	④ Desolved components	$\nabla\left(\frac{Kkr_{cw}R_{cw}}{\mu_{cw}B_{cw}}\nabla\Psi_{cw}\right)+\nabla\left(D_{cw}\nabla\frac{R_{cw}}{\alpha_{cw}}\right)-q_{cS}^{cw}+f_{cS}^{cc-cw}+f_{caS}^{ca-cw}-f_{cS}^{cw-r}=\frac{\partial}{\partial t}\left(\phi\frac{S_{cw}R_{cw}}{B_{cw}}\right)$
	⑤ Volatile components	$\nabla\left(\frac{Kkr_{ca}R_{ca}}{\mu_{ca}B_{ca}}\nabla\Psi_{ca}\right)+\nabla\left(D_{ca}\nabla\frac{R_{ca}}{\alpha_{ca}}\right)-q_{cS}^{ca}+f_{cS}^{ca-cc}-f_{caS}^{ca-cw}=\frac{\partial}{\partial t}\left(\phi\frac{S_{ca}R_{ca}}{B_{ca}}\right)$
Energy conservation	⑥ Fluid	$\nabla\left(\rho_{cw}\frac{Kkr_{cw}H_{cw}}{\mu_{cw}}\nabla\Psi_{cw}\right)+\nabla\left(\rho_{ca}\frac{Kkr_{ca}H_{ca}}{\mu_{ca}}\nabla\Psi_{ca}\right)+\nabla\left(\rho_{cc}\frac{Kkr_{cc}H_{cc}}{\mu_{cc}}\nabla\Psi_{cc}\right)$ $-\rho_{wS}q_{wS}H_{cw}-\rho_{caS}q_{gS}H_{ca}-\rho_{ccS}q_{cS}H_{cc}+\nabla\cdot(\lambda_f\nabla T_f)-f_{f\rightarrow r}=\frac{\partial}{\partial t}(\rho_w\phi S_{cw}U_{cw}+\rho_{ca}\phi S_{ca}U_{ca}+\rho_{cc}\phi S_{cc}U_{cc})$
	⑦ Solid	$\nabla\cdot(\lambda_f\nabla T_f)-f_{r\rightarrow f}=\frac{\partial}{\partial t}(\rho_r(1-\phi)U_r)$

Figure 10 shows calculated and observed temperature profiles in wells. The positions of the observation wells are indicated in Figure 11. Simulated profiles generally match with observed ones.

Subsurface water flow system at the Sendai plain is thus reconstructed by the matching of calculated and observed temperature profiles at observation wells and water levels at the wells, rivers, lakes and sea. The resultant temperature distribution at a depth of -40m is shown in Figure 12. Temperature distribution of the overall area is thus obtained by the numerical simulation in a manner far better than a geometrical interpolation of the temperature data.

Although distance between recharge and discharge zones are rather short in the Sendai plain, temperature difference caused by groundwater flow is clearly shown in Figure 12. The temperature along the coast in the east is higher than that on mountainous region in the west, up to 2.5 K.

Table 2. Physical property values used for the simulation

Absolute permeability	Quarternary : 2×10^{-11} (m^2) Tertiary : 1×10^{-15} (m^2) ←function of depth
Effective porosity	Quarternary : 20 (%) Tertiary : 10 (%) ←function of depth
Heat conductivity	Rock: Quarternary 0.93 (W/m･K), Tertiary 1.20 - 1.70 (W/m･K) Water: 0.561 (W/m･K) Air: 0.0241 (W/m･K) Fluid: function of water saturation
Heat capacity	Rock: 0.96 (kJ/kg･K) Heat capacity of fluid is a function of temperature
Rock density	2500 (kg/m^3)
Atmospheric temperature	14.5 °C (meteorological data at Sendai)
Precipitation	1.71 (mm/d) (meteorological data at Sendai)
Boundary condition of temperature	Surface: precipitation (atmospheric temperature) Bottom: 79°C(constant) Side: thermally insulated
Initial thermal gradient	0.03 (°C /m)

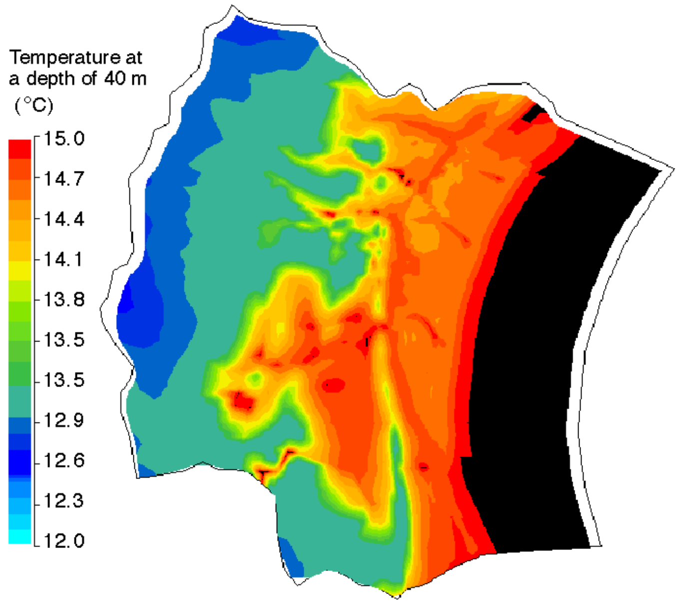

Figure 12. Calculated subsurface temperature distribution.

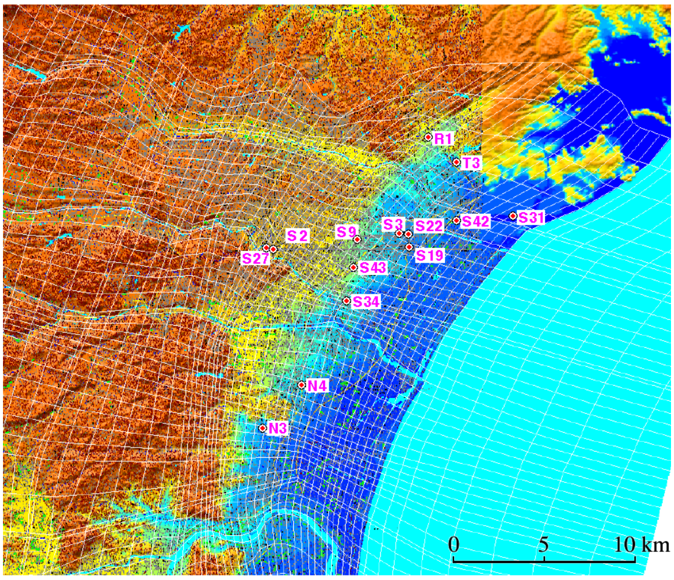

Figure 11. Observation wells for temperature matching

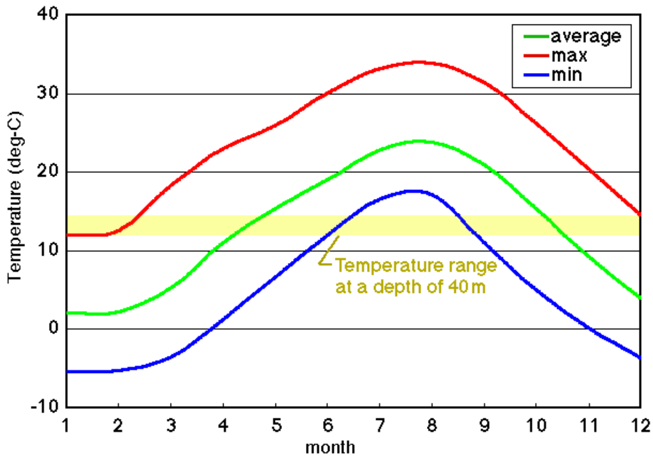

Figure 13. Atmospheric temperature in Sendai.

Figure 13 shows the atmospheric temperature change at Sendai city (average, 1999-2003). Subsurface temperature at a depth of 40 m (12-15°C) is higher than atmospheric temperature in the winter and lower in the summer. Therefore in this area, geothermal heat-pump meet the demands of both space heating and cooling.

4. TEMPERATURE MEASUREMENT IN THAILAND

As an example of tropical climate region, temperature measurement at the basins along the Chao-Phraya river, Thailand is introduced in this section. For these areas, possibility of geothermal heat-pump system for space cooling is investigated.

Location of observation wells in this area, for which temperature profiles are obtained, are shown in Figure 14. Northern 6 wells are located in the upper basin of the Chao-Phraya river, while southern ones are in the lower basin.

Figure 15 shows the observed Observed temperature profiles for these wells. Generally the wells in the upper basin have lower subsurface temperature than the ones in the lower basin. However, GWA0041 and GWA0076 in the lower basin has rather low temperatures and the type of their profiles are that of recharge zone. Therefore, these wells are considered to be located in local recharge zones of the lower basin for shallow groundwater flow. Shallow local flows may exist in upper and lower basins, respectively.

Figure 16a and 16b shows the atmospheric temperature at Bangkok and Udon Thani, respectively. Since elevation of Udon Thani is higher than that of upper basin, its subsurface temperature may be approximately same or even lower than upper basin. Yellow belts in Figure 16a and 16b shows the assumed temperature at a depth of 40 m based on Figure 15. In Bangkok, there is no thermal merit of geothermal heat-pump for space cooling because subsurface temperature is approximately same level as maximum atmospheric temperature. On the other hand in Udon Thani, subsurface temperature is approximately same as the average atmospheric temperature and it is lower than maximum temperature. Therefore, at Udon Thani, there may be a thermal merit of geothermal heat-pump system in daytime use.

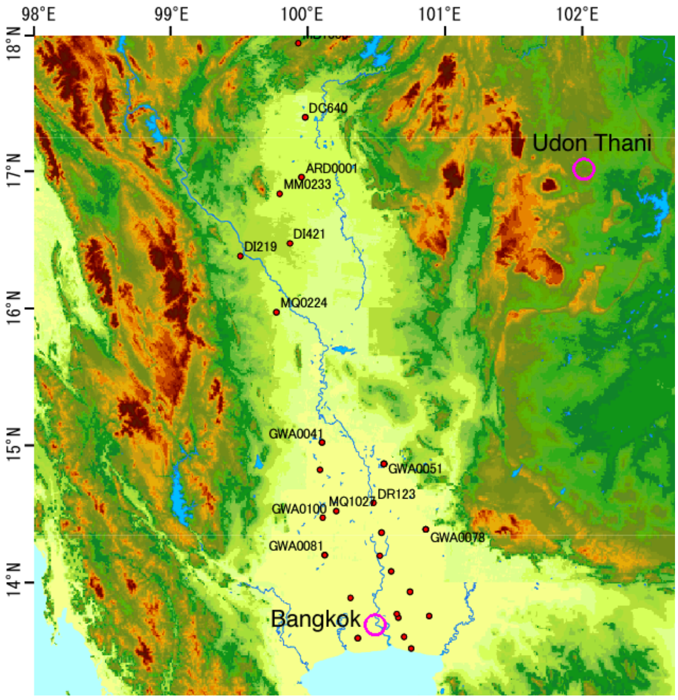

Figure 14. Observation well locations in Thailand.

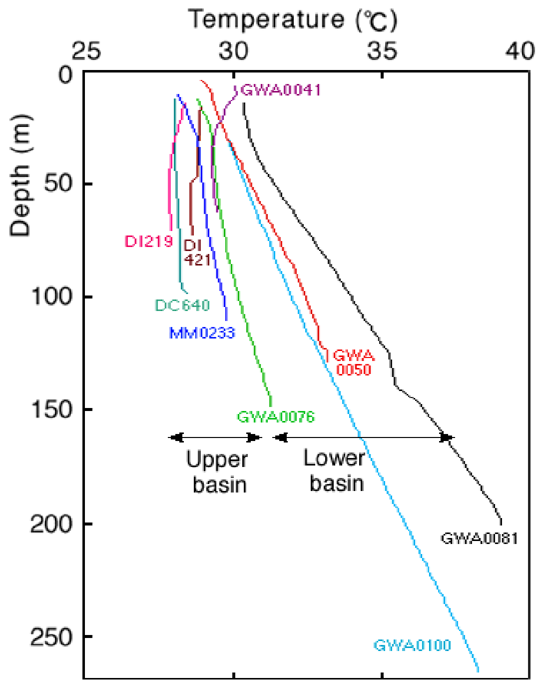

Figure 15. Observed temperature profiles in Thailand.

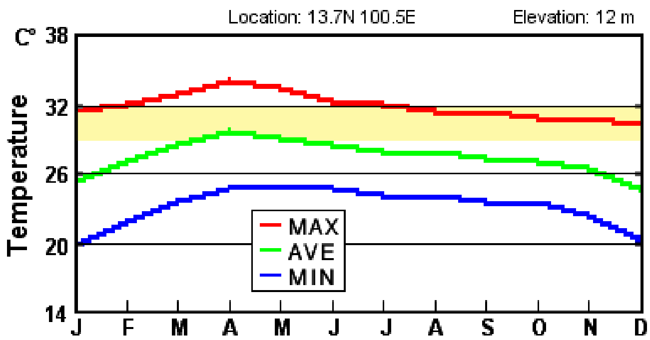

Figure 16a. Atmospheric temperature at Bangokok.

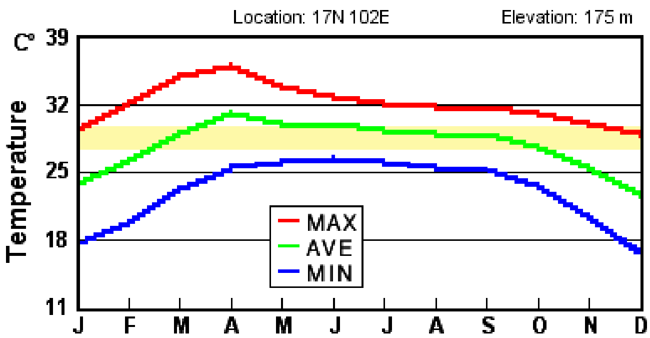

Figure 16b. Atmospheric temperature at Udon Thani.

5. FUTURE PLANS

We are planning to measure temperature and also get samples for chemical and isotopic analysis for wells in Thailand (additional) and Vietnam this fiscal year. Compilation of existing well data in various areas is also needed. Our future plan is to reconstruct (numerical) models of groundwater flow system in major plains in East Asia to obtain temperature contour map for a depth that can be used for heat-exchange. The final goal is to make potential map of heat resources for geothermal heat-pump application, showing the criteria of heating, cooling, both, and none, due to the balance between surface and subsurface temperature conditions.

6. CONCLUSIONS

Subsurface temperature distribution in layers shallower than the basement in the Sendai plain was obtained by field measurement and numerical modeling of the groundwater flow. Since subsurface temperature is lower than summer atmospheric temperature but lower than winter one in this area, geothermal heat-pump can be applied for both space heating and cooling. Results of temperature measurement in the wells in Thailand suggest a possibility of geothermal heat-pump application for space heating at upper basin, but not for lower basin. Thus the possible potential geothermal heat-pump application at any location can be judged by comparing the subsurface temperature with atmospheric temperature.

ACKNOWLEDGEMENTS

The study at the Sendai plain was done as a part of "Geological Research for utilization of low-temperature geothermal resources" sponsored by NEDO (FY2001-2003). The numerical simulation of the Sendai plain by GETFLOWS was conducted by Geosphere Environmental Technology Corporation. The temperature measurement in Thailand is conducted by co-operation with Department of Mineral Resources, Thailand.

REFERENCES

Mori, K., Tosaka, H., Uchida, Y., Yasukawa, K. and Ohtani, T. (2003) 3-Dimensional Surface/Subsurface water and heat flow simulation system, 2003 Annual meeting Geothermal Society of Japan, 56 (in Japanese).

Uchida Y. and Sakura, Y. (1999) Subsurface temperature profiles in the Nobi Plain, central Japan. *Bull. Geol. Surv. Japan*, **50** (10), 635-659 (in Japanese with English abstract).

Uchida, Y., Tenma, N., Yasukawa, K., Ohtani, T. And Mori, K. (2005?) Case study for the direct utilization of geothermal energy at the Sendai plains 1) Construction of 3D Regional groundwater flow and heat transport model. *Jour. Geothermal Research Association Japan* (submitted, in Japanese with English abstract)